CEA/DAPNIA/SEA-98-04

Multi-bunch experiments on TTF

Stéphane Fartoukh
DAPNIA/SEA,
CEA/Saclay F-91191 Gif sur Yvette Cedex, France

February 23, 1998

Abstract

The goal of this paper is to discuss and simulate two beam experiments already proposed for the future runs of TTF with Injector II and concerning the multi-bunch beam breakup instability induced by the dipole modes of TESLA cavities.

1 Introduction and experimental protocol

The beam breakup phenomenon caused by the long-range dipole wakefields is theoretically well-controlled in the TESLA linac through a mode damping combined with a large bunch spacing on the one hand and the natural cavity to cavity mode detuning on the other hand (real cavities with the same fundamental frequency have different frequencies of higher harmonics due to manufacturing defects). However, contrary to the eigenfrequencies ω_i and to the ratios $\left(R/Q\right)_i$ of dipole modes, the decay times $T_{f_i} = 2\,Q_i/\omega_i$ of the latter are known with a poor accuracy (since they depend on the dissipative environment of the cavity within the linac) or not known at all for the trapped modes. Two different experiments based on beam measurements in the TTF linac have then been proposed to estimate the quality factors Q_i associated to the most dangerous dipole modes of TESLA cavities. They are described hereafter.

The first one (Experiment I) consists in injecting the beam off-axis into the first non-powered 8-cavity module and monitoring the bunch positions at its exit (see Fig. 1, A. Mosnier [1, p. 358]). If one of the transverse modes verifies the resonance condition [2],

$$\omega_i = n\,\omega_b\,(1 \pm 1/2Q_i)\ , \tag{1}$$

where n is integer and where $\omega_b/2\pi$ represents the bunch repetition frequency, then the transverse beam displacement is amplified at the BPM location by an amount which is proportional to the initial offset δx_0, the bunch charge Q_b and the shunt impedance R_i of the selected mode:

$$\delta x_{\mathrm{BPM}} - \delta x_0 = \mathbf{Cst_1}\ \times\ \delta x_0\, Q_b\, R_i\ . \tag{2}$$

Note that the tuning system can be actuated in order to obtain the resonance condition introduced above since the cavities are not powered for this experiment and since the bunch repetition frequency will be equal to 1 MHz with Injector II.

For the second experiment proposed (Experiment II), it is a matter of modulating with time the initial transverse coordinates of the bunches at the frequency $\Omega/2\pi$ (V. Balakin [3]). By operating with a pair of rf deflectors (see Fig. 2), the bunch number k goes into the first cryomodule with the following initial conditions:

$$\delta x_{k,0} = \delta x_0\ \sin(k\,\Omega\,T + \phi)\ \ \text{and}\ \ \delta x'_{k,0} = 0 \tag{3}$$

where $T \stackrel{\mathrm{def}}{=} 2\pi/\omega_b$ and $0 \le \Omega < \omega_b$ (first Brillouin zone). Considering the dipole mode number i and writing the eigenfrequency ω_i as $\omega_i = \omega_b\,(n_i + \eta_i)$ where $-0.5 < \eta_i \le 0.5$ (n_i being the integer closest to the ratio ω_i/ω_b), we will see that resonances occurs when the following condition is satisfied:

$$\Omega = \omega_b\,|\eta_i|\ \ \text{or}\ \ \Omega = \omega_b\,(1 - |\eta_i|)\ . \tag{4}$$

If this condition is checked, we will show that the output BPM signal possesses a component in quadrature with respect to the input signal, the amplitude of which is proportional to the amplitude δx_0, the bunch charge Q_b and the shunt impedance R_i:

$$\delta x_{k,\mathrm{BPM}} - \delta x_{k,0} = \mathbf{Cst_2}\ \times\ \delta x_0\, Q_b\, R_i\ \cos(k\,\Omega\,T + \phi)\ . \tag{5}$$

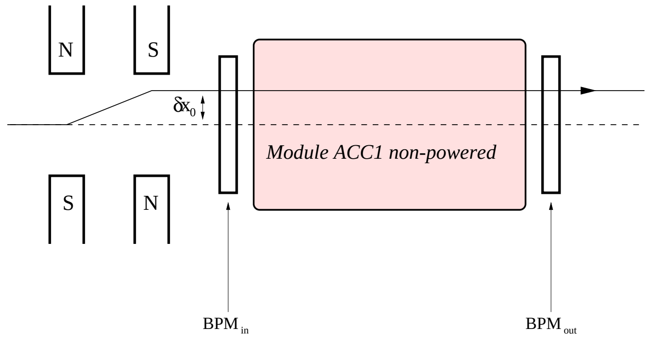

Figure 1: Experiment I

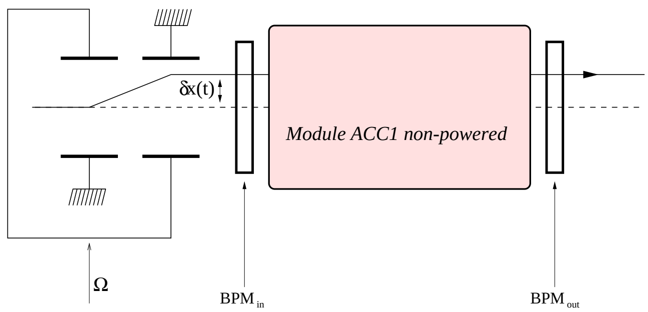

Figure 2: Experiment II

Thus, by varying Ω between 0 and $\omega_b/2$ (i.e. between 0 and 0.5 MHz considering the Injector II beam parameters), one can theoretically scan all the frequencies of the most dangerous dipole modes (i.e possessing the highest impedances). Note also that the cavities have to be un-powered for this experiment in order to maximize the signal amplitude obtained at the BPM location.

In conclusion and in view of Eqs. 2 and 5, these two experiments permit to estimate **individually** the quality factors Q_i of the highest impedance dipole modes if we consider that the ratios R_i/Q_i are known for each of them (simulation with URMEL or direct measurements [1, p. 135]) and provided that two different modes i and j do not verify the following condition:

$(\omega_j - \omega_i)/\omega_b$ integer for Experiment I
$(\omega_j - \omega_i)/\omega_b$ or $(\omega_j + \omega_i)/\omega_b$ integer for Experiment II.

Note finally that the constants $\mathbf{Cst_1}$ and $\mathbf{Cst_2}$ appearing in Eqs. 2 and 5 are identical, as will be shown in Section 3; from this point of view, the measurement methods I and II possess exactly the same sensitivity (under the condition that $\delta x_0^{Exp.I} = \delta x_0^{Exp.II}$, see Eqs. 2 and 5).
After some recalls of beam dynamics (Section 2), we will derive in Section 3 the resonance conditions described by Eqs. 1 and 4 and give the associated amplification factors ($\mathbf{Cst_1}$ or $\mathbf{Cst_2}$); finally, in Section 4, we will simulate the two experiments previously described.

2 Basic equations in multi-bunch operation

2.1 Equation of motion

Let us consider a train of N electron bunches separated by a distance $\lambda_b = cT = 2\pi c/\omega_b$ and traveling across rf accelerating structures and magnetic quadrupoles. We note s the longitudinal coordinate along the beam line and z the relative position of particles within the train satisfying the following two conditions: $z = 0$ at the center of the first bunch and $z > 0$ at the train tail. We will assume the train to be fully relativistic so that the longitudinal charge distribution $\rho(z)$ is not distorted by the beam transport:

$$\rho(z) = \sum_{k=0}^{N-1} \rho_0(z - k\lambda_b)$$

where ρ_0 denotes the charge distribution of the first bunch. For a slice of charge at a relative position z inside the train, we note $\delta x(s,z)$ the transverse position (horizontal or vertical) of its center of mass, $x(s,z) = \delta x(s,z) + \tilde{x}(s,z)$ the position of any particle within the slice considered and $\gamma(s,z)mc^2$ its energy (thus, $\tilde{x}$ describes the betatron motion in the presence of acceleration). The fundamental dynamics equation, projected on the transverse and longitudinal planes, gives [4]:

$$\begin{cases} x''(s,z) + \dfrac{\gamma'(s,z)}{\gamma(s,z)}\, x'(s,z) + k(s,z)\, x(s,z) = \dfrac{e}{\gamma(s,z)mc^2} \displaystyle\int_{-\infty}^{z} W_T^{\delta}(z-z^*)\rho(z^*)\delta x(s,z^*)\, dz^* \\ \gamma'(s,z) = e/mc^2 \Big(G_{\mathrm{rf}}(s,z) - \displaystyle\int_{-\infty}^{z} \rho(z^*)\, W_L^{\delta}(z-z^*)\, dz^* \Big) \end{cases} \tag{6}$$

where the derivatives are taken with respect to s. Here, W_L^δ and W_T^δ are the longitudinal and transverse delta-function wake potentials, $k(s,z)$ [m^{-2}] is the quadrupole strength seen by the slice z and $G_{\mathrm{rf}}(s,z)$ [V/m] represents the rf accelerating gradient all along the line[1]. We restrict now the equation of motion 6 to the beam transport through a non-powered accelerating structure ($G_{\mathrm{rf}}(s,z) = k(s,z) = 0$) and suppose that the eigenfrequency of the fundamental monopole mode is not an integer multiple of the bunch repetition frequency (detuned cavity): therefore, the multi-bunch beam-loading can be neglected and, in a more general way, the beam energy can be assumed constant all along the structure, equal to its initial value E_0. Summing Eq. 6 over all the particles of the slice z, we obtain the equations verified by the quantities $\delta x(s,z)$ and $\tilde{x}(s,z)$:

$$\delta x''(s,z) = \frac{e}{E_0} \int_{-\infty}^{z} W_T^\delta(z-z^*)\, \rho(z^*)\, \delta x(s,z^*)\, dz^* \tag{7}$$

and $\tilde{x}''(s,z) = 0$ (Hill equation in a drift space).
The simulation results which will be shown in Section 4 are based on a numerical integration of Eq. 7, including the effects of wakefields over the finite bunch length (short-range

[1] $G_{\mathrm{rf}}(s,z) = 0$ and $k(s,z) = G_q(s)e/(\gamma(s,z)mc)$ in quadrupoles, $G_q(s)$ [T/m] being the step function which describes the quadrupole gradient within the line; $k(s,z) = eG'_{\mathrm{rf}}(s,z)/\big(2\,\gamma(s,z)mc^2\big)$ in accelerating structures (rf focusing effects, see Ref. [5] for more details).

wakefields). Nevertheless, in order to go further in the analytical treatment of the problem, we have to make the two following assumptions:

- each bunch is considered as a point-like charge Q_b so that the longitudinal charge distribution is given by the expression $\rho(z) = Q_b \sum_{k=0}^{N-1} \delta(z - k\lambda_b)$.
- only the long-range dipole wakefields are taken into account.

Under these simplifications, Eq. 7 becomes

$$\delta x_n''(s) \;=\; \frac{e\,Q_b}{E_0} \sum_{k=0}^{n} W_T\Big((n-k)\,\lambda_b\Big)\,\delta x_k(s)\ ,\ n = 0\ldots N-1 \tag{8}$$

where $\delta x_n(s) \stackrel{\text{def}}{=} \delta x(s, n\lambda_b)$ describes the transverse displacement of bunch number n and where W_T [V/C/m^2] represents the long-range dipole wakefield per unit length and unit charge:

$$\begin{array}{l} W_T(z) = 2 \displaystyle\sum_{i\in modes} \frac{k_i\,c}{\omega_i\,a^2} \sin(\omega_i z/c)\ \exp(-z/z_i)\ , z > 0 \\ \text{with} \left\{ \begin{array}{lll} k_i \stackrel{\text{def}}{=} \dfrac{\omega_i}{4}\left(\dfrac{R}{Q}\right)_i & & \text{(loss factor per unit structure length [V/C/m])} \\ z_i \stackrel{\text{def}}{=} c\,\dfrac{2\,Q_i}{\omega_i} & & \text{(damping length [m] of mode } i) \end{array} \right. \end{array} \tag{9}$$

where a is the iris aperture radius.

2.2 Methods of resolution

The simplified equation of motion 8 can be solved analytically by considering the Z-transform [6] of the function set $\{\delta x_n(s)\}_n$:

$$\left\{ \begin{array}{lll} \Big\{\delta x_n(s)\Big\}_n & \stackrel{\mathrm{Z}}{\longrightarrow} & \delta\tilde{x}(s,Z) \stackrel{\text{def}}{=} \displaystyle\sum_{n=0}^{\infty} \delta x_n(s)\, Z^n \\ \delta\tilde{x}(s,Z) & \stackrel{\mathrm{Z}^{-1}}{\longrightarrow} & \Big\{\delta x_n(s)\Big\}_n = \left\{ \dfrac{1}{n!} \left(\dfrac{\partial^n \delta\tilde{x}}{\partial Z^n}\right)_{Z=0} \right\}_n \end{array} \right. . \tag{10}$$

The Z-transform of the wakefield force (right-hand term of Eq. 8) is then, from the convolution theorem, the product of $\delta\tilde{x}$ by the Z-transform of the wake potential noted $\widetilde{W}_T$:

$$W_T \stackrel{\mathrm{Z}}{\longrightarrow} \widetilde{W}_T(Z) \stackrel{\text{def}}{=} \sum_{n=0}^{\infty} W_T(n\lambda_b)\, Z^n = 2 \sum_i \frac{k_i\,c}{\omega_i\,a^2}\ \frac{\sin(\omega_i T)}{Z\,e^{-\lambda_b/z_i} + Z^{-1}\,e^{\lambda_b/z_i} - 2\ \cos(\omega_i T)}\ .$$

After these transformations, Eq. 8 becomes then a classical linear differential equation of second order which can be solved analytically:

$$\delta\tilde{x}''(s,Z) - \frac{e\,Q_b}{E_0}\,\widetilde{W}_T(Z)\,\delta\tilde{x}(s,Z) = 0 \quad\Rightarrow$$
$$\delta\tilde{x}(s,Z) = \delta\tilde{x}(0,Z)\,\cosh\Bigl(f(Z)\,s\Bigr) + \delta\tilde{x}'(0,Z)\,\frac{\sinh\Bigl(f(Z)\,s\Bigr)}{f(Z)} \text{ with } f(Z) \stackrel{\text{def}}{=} \sqrt{\frac{e\,Q_b}{E_0}\,\widetilde{W}_T(Z)}\,,$$

where the functions $x \mapsto \cosh(\sqrt{x})$ and $x \mapsto \sinh(\sqrt{x})/\sqrt{x}$ has to be defined by their analytical series.
All the difficulties come now from the computation of the inverse Z-transform (see Eq. 10) of the formal solution given above. This is done in Ref. [2] for initial conditions which are the ones of Experiment I, i.e $\delta x_{n,0} = \delta x_0$ and $\delta x'_{n,0} = 0$ (giving $\delta\tilde{x}(0,Z) = \delta x_0/(1-Z)$ and $\delta\tilde{x}'(0,Z) = 0$). Concerning the initial conditions of the bunch train which relative to Experiment II (see Eq. 3), the computations become rapidly inextricable and we prefer to make the following approximation: at the exit of the cavity of length L, the bunch number n have been simply affected by a kick given by:

$$\begin{aligned}\delta x'_n(L) &= \frac{eQ_b}{E_0}\sum_{k=0}^{n} W_T\Bigl((n-k)\lambda_b\Bigr)\int_0^L \delta x_k(s)\,ds \approx \frac{eQ_b}{E_0}\,L\sum_{k=0}^{n} W_T\Bigl((n-k)\lambda_b\Bigr)\,\delta x_{k,0}\\ &\approx \delta x_0\frac{eQ_b}{E_0}\,L\sum_{k=0}^{n} W_T\Bigl((n-k)\,\lambda_b\Bigr)\sin(k\Omega T+\phi)\ .\end{aligned} \tag{11}$$

Note that the preceding relations hold also for Experiment I, by replacing Ω with zero and ϕ by $\pi/2$.

3 Steady-state regime, resonance conditions, amplification coefficients

3.1 Steady state regime

It is now matter of computing the sum appearing in the right-hand side of Eq. 11. After a transient regime associated to the maximum damping length of the highest impedance dipole modes (about 150 bunches for TESLA), the bunches reach again a steady configuration within the train. After some algebra, we obtain for this regime:

$$\begin{aligned}\delta x'_N(L) \stackrel{N\to\infty}{\approx} \delta x_0\,L\,\frac{eQ_b}{E_0}\,\frac{c}{2a^2}&\left\{\left[\sum_i\left(\frac{R}{Q}\right)_i\mathcal{A}_+(\omega_i,Q_i,T,\Omega)\right]\sin(N\Omega T+\phi)-\right.\\ &\left.\left[\sum_i\left(\frac{R}{Q}\right)_i\mathcal{A}_-(\omega_i,Q_i,T,\Omega)\right]\cos(N\Omega T+\phi)\right\}\\ = \delta x_0\,L\,\frac{eQ_b}{E_0}\,\frac{c}{2a^2}&\sum_i\left(\frac{R}{Q}\right)_i\mathcal{A}(\omega_i,Q_i,T,\Omega)\sin\Bigl(N\Omega T+\phi-\varphi(\omega_i,Q_i,T,\Omega)\Bigr)\end{aligned} \tag{12}$$

where the response functions $\mathcal{A}_\pm$ and $\mathcal{A}$ as well as the phase shift φ are defined hereafter:

$$
\begin{aligned}
\mathcal{A}_+(\omega,Q,T,\Omega) &\stackrel{\text{def}}{=} \frac{1}{2}\,\frac{\sin(\omega T)\left(\cosh\left(\frac{\omega T}{2Q}\right)\cos(\Omega T)-\cos(\omega T)\right)}{\left(\cosh\left(\frac{\omega T}{2Q}\right)-\cos(\omega T-\Omega T)\right)\left(\cosh\left(\frac{\omega T}{2Q}\right)-\cos(\omega T+\Omega T)\right)} \\
\mathcal{A}_-(\omega,Q,T,\Omega) &\stackrel{\text{def}}{=} \frac{1}{2}\,\frac{\sin(\omega T)\,\sinh\left(\frac{\omega T}{2Q}\right)\,\sin(\Omega T)}{\left(\cosh\left(\frac{\omega T}{2Q}\right)-\cos(\omega T-\Omega T)\right)\left(\cosh\left(\frac{\omega T}{2Q}\right)-\cos(\omega T+\Omega T)\right)} \\
\mathcal{A}(\omega,Q,T,\Omega) &\stackrel{\text{def}}{=} |\mathcal{A}_+ + i\mathcal{A}_-| = \sqrt{{\mathcal{A}_+}^2+{\mathcal{A}_-}^2} \\
\varphi(\omega,Q,T,\Omega) &\stackrel{\text{def}}{=} \arg(\mathcal{A}_+ + i\mathcal{A}_-) \in [-\pi,\pi[\ .
\end{aligned}
\tag{13}
$$

3.2 Experiment II

For a given dipole mode (ω and Q fixed) and a given bunch spacing $\lambda_b = cT$, these functions are of period $\omega_b = 2\pi/T$ with the modulation frequency Ω; $\mathcal{A}_+$ and $\mathcal{A}_-$ are symmetrical and anti-symmetrical respectively with respect to $\omega_b/2$. It is then sufficient to study their variations for frequencies Ω between 0 and $\omega_b/2$ (i.e 0–0.5 MHz for TESLA) and, as we are going to see, the response function $\mathcal{A}$ presents a very narrow resonance in this frequency range. By writing the eigenfrequency of the selected mode as $\omega = \omega_b(n+\eta)$ with n integer and $\eta \in]-0.5, 0.5[/\{0\}$ [2], the behavior of the amplitudes $\mathcal{A}_\pm$ between 0 and $\omega_b/2$ is summarized hereafter:

- the function $\mathcal{A}_-$ reaches its peak value, $\mathcal{A}_-^{peak} = \epsilon_\eta\, Q/(2n\pi)$, at $\Omega = \omega_b(|\eta| + \bigcirc(1/Q^4))$, where ϵ_η represents the sign of η, and is vanishing for $\Omega = 0$ and $\Omega = \omega_b/2$.
- inversely, the amplification $\mathcal{A}_+$ is zero at $\Omega = \omega_b(|\eta| + \bigcirc(1/Q^2))$ and possesses two extrema, $\mathcal{A}_+^{peak} = \mp\,\epsilon_\eta\, Q/(4n\pi)$, for $\Omega = \omega_b(|\eta| \pm n/(2Q) + \bigcirc(1/Q^3))$ respectively; the values of $\mathcal{A}_-$ at these two points are $\mathcal{A}_-^{peak}/2 = \epsilon_\eta\, Q/(4n\pi)$.

Therefore, the complete amplitude $\mathcal{A}$ exhibits a resonance for $\Omega \approx |\eta|$, $\mathcal{A}^{peak} = |\mathcal{A}_-^{peak}| = Q/(2n\pi)$, with a width $\Delta\Omega \sim n\omega_b/Q \sim \omega/Q$ corresponding to the bandwidth of the selected mode. The behavior of these functions is summarized in Tab. 1 and they are plotted in Fig. 3, considering the most dangerous dipole mode of TESLA cavities (mode TM_{110}, $\omega = 2\pi \times 1873.84$ MHz and $Q = 1.2\,10^5$, giving $\eta = -0.16$ for $T = 1\mu$s).

In brief, assuming the dipole wake to be strongly dominated by few resonant modes (modes TE_{111} and TM_{110} for the TESLA cavities) and supposing that the latter do not overlap in the frequency domain (in the sense where the sum and difference of frequencies

[2] If $\eta = 0$ or $\eta = \frac{1}{2}$ (zero-crossings), then $\mathcal{A}_+ = \mathcal{A}_- = 0$.

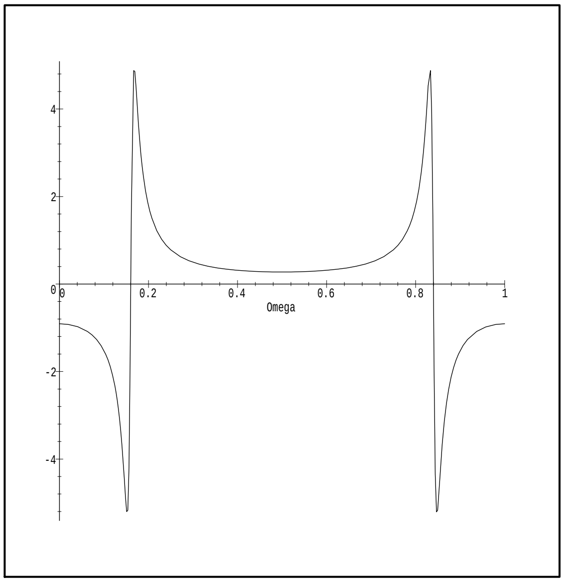

$\mathcal{A}_+$ vs $\Omega/2\pi$ [MHz]

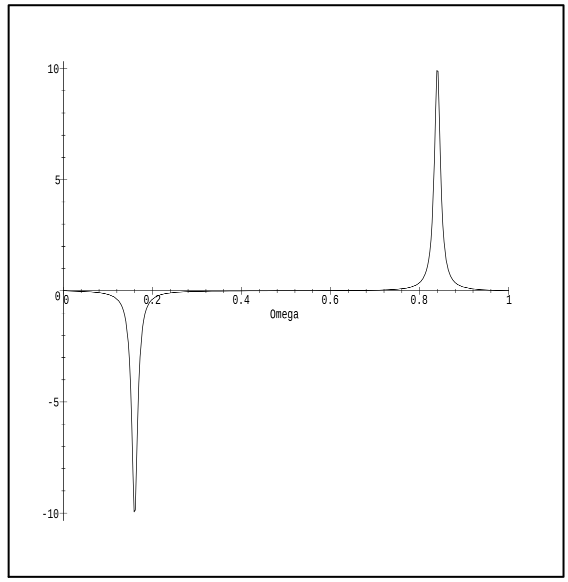

$\mathcal{A}_-$ vs $\Omega/2\pi$ [MHz]

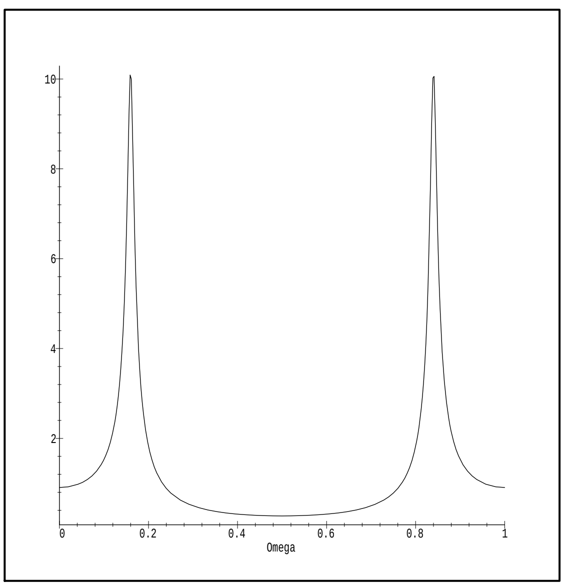

$\mathcal{A}$ vs $\Omega/2\pi$ [MHz]

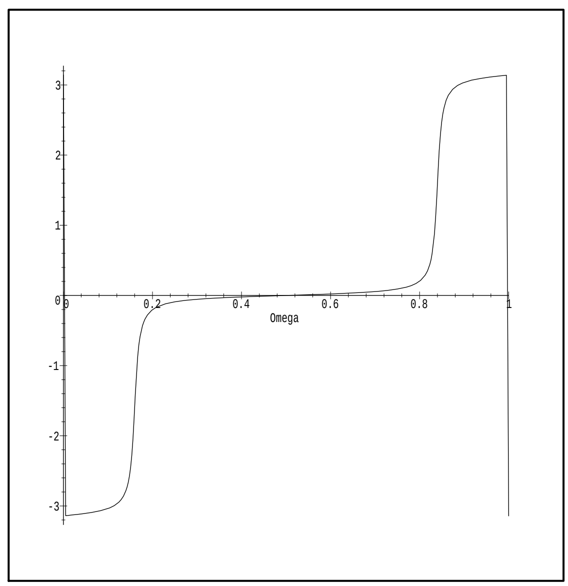

φ [rad] vs $\Omega/2\pi$ [MHz]

Figure 3: Selection of the TM_{110} mode at $\omega/2\pi \sim 1875$ MHz ($Q = 1.2\,10^5$ and $\eta = -0.16$)

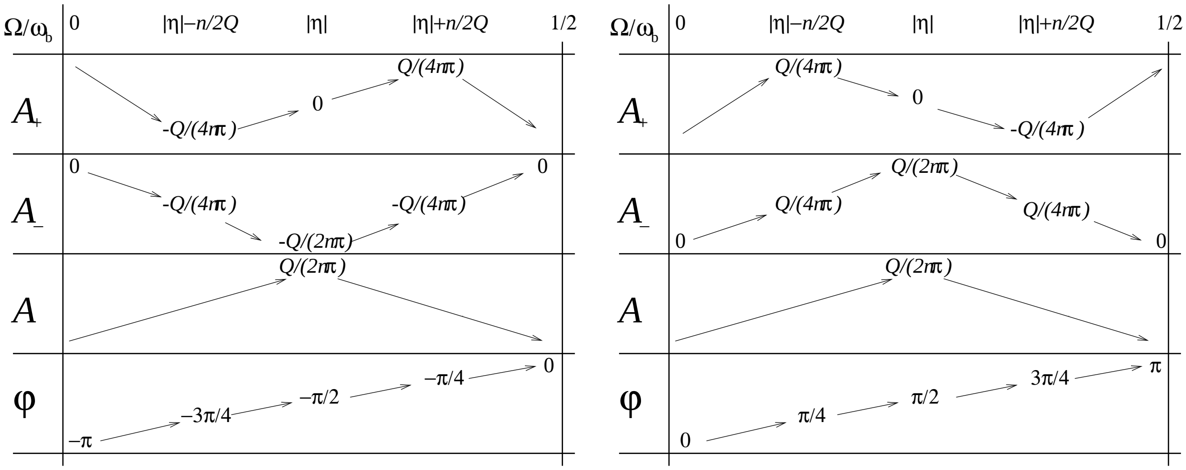

Case $\eta < 0$ Case $\eta > 0$

Table 1: Behavior of the functions $\mathcal{A}_{\pm}$, $\mathcal{A}$ and φ for Ω between 0 and $\omega_b/2$

of two of these modes are not an integer multiple of the bunch repetition frequency), then, if the ratio Ω/ω_b is chosen equal to the coefficient$|\eta|$ associated to one of them, the output signal possesses a component in quadrature of phase with respect to the input one, which is given by the following expression:

$$\delta x_{k,\mathrm{BPM}} - \delta x_{k,0} = \underbrace{\delta x_0\, L_{\mathrm{cav}\to\mathrm{BPM}} \times \frac{eQ_b}{E_0} \times \frac{c}{2a^2}\left(\frac{R}{Q}\right) L_{\mathrm{cav}} \times \frac{Q}{2\pi\omega/\omega_b}}_{\stackrel{\mathrm{def}}{=}\delta x_{\mathrm{BPM}}} \times \cos(k\,\Omega\,T + \phi)\ . \quad (14)$$

We obtain $\delta x_{\mathrm{BPM}} \approx \delta x_0/2$ for bunches of charge $Q_b = 8\,\mathrm{nC}$ and input energy $E_0 = 20\,\mathrm{MeV}$ and for the TM_{110} mode at 1875 MHz ($\omega/\omega_b \approx 1875$, $L_{\mathrm{cav}}(R/Q)/a^2 \approx 8.6\,10^4\,\Omega/\mathrm{m}^2$ and $Q \approx 1.2\,10^5$) selected in the first cavity of module ACC1 ($L_{\mathrm{cav}\to\mathrm{BPM}} \approx 10\,\mathrm{m}$).

3.3 Experiment I

As said previously, the computation of amplitudes $\mathcal{A}_{\pm}$ holds also when the initial conditions of bunches are the one required for Experiment I. These initial conditions can be obtained from Eq. 3 by replacing Ω with zero and ϕ by $\pi/2$, so that $\mathcal{A}_-$ is vanishing in this case and the component $\mathcal{A}_+$ takes the simplified following form (identical to the response function p_r given in Ref. [2]):

$$p_r(\omega) \stackrel{\mathrm{def}}{=} \mathcal{A}_+(\omega, Q, T, \Omega = 0) = \frac{1}{2}\,\frac{\sin(\omega T)}{\cosh\left(\dfrac{\omega T}{2Q}\right) - \cos(\omega T)}\ . \quad (15)$$

This function reaches its peak values $p_r^{peak} = \pm Q/(2n\pi)$ at $\omega = n\omega_b(1 \pm 1/(2Q))$ and is vanishing at the zero-crossings, $\omega = n\omega_b$ and $\omega = n(\omega_b + 1/2)$ (see Fig. 4). Therefore, by actuating the tuning system of a given cavity within the first cryomodule, the measurements done at BPM should exhibits resonances of the same width and amplitude as the one previously described; more precisely and according to the numerical application made in the previous subsection, the contribution of long-range dipole wakes to the beam displacement at the BPM location is about $\delta x_0/2$ for a bunch charge of 8 nC and when only the first cavity of module ACC1 is tuned to the TM_{110} mode at 1875 MHz.

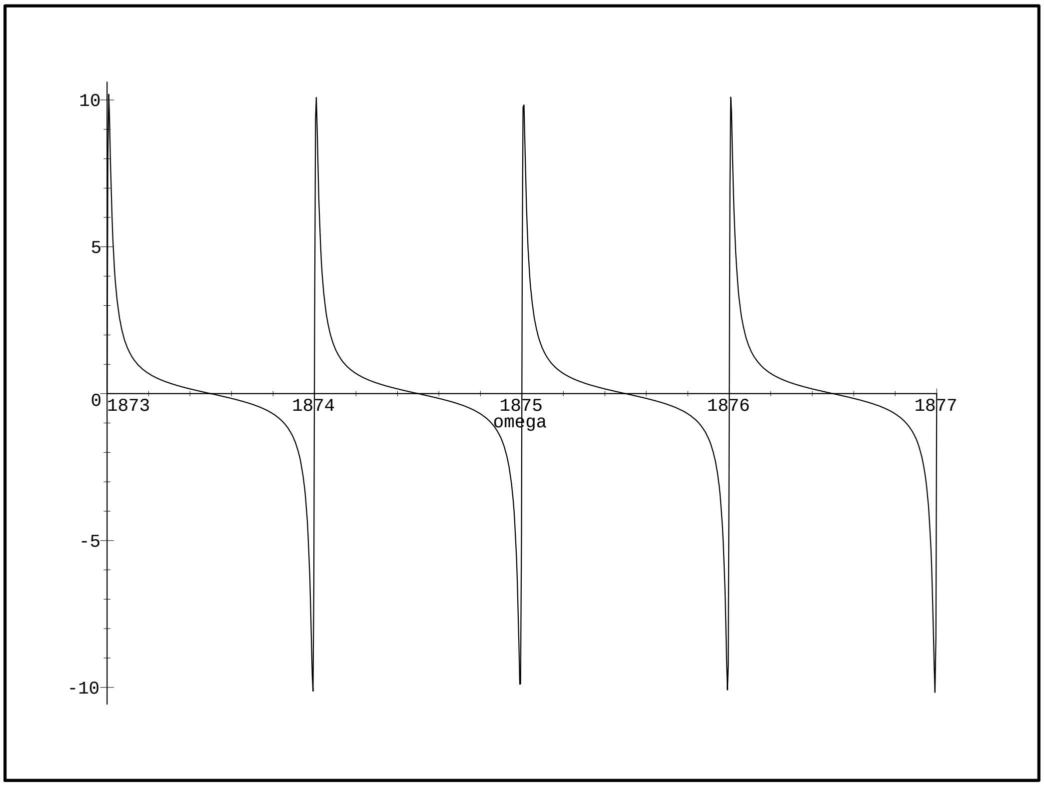

Figure 4: p_r vs $\omega/2\pi$ in the range 1873–1877 MHz (with $Q = 1.2\,10^5$)

4 Simulation results

Ten dipole modes with an rms frequency spread of 1 MHz (from cavity to cavity) have been used in order to construct the long-range dipole wake potential generated in the TESLA cavities. In this model, the two experiments have been simulated for bunches of charge Q_b equal to 1.6 or 8 nC, of length $\sigma_z = 1$ mm and injected at the energy $E_0 = 20.511$ MeV (beam parameters for Injector II); the quantity δx_0 has been chosen equal to 10 mm for each of these experiments (i.e the initial bunch train displacement for Experiment I or the transverse modulation amplitude of the train after the rf deflectors for Experiment II). Finally, the results shown in the next two subsections have been obtained either by artificially switching off the short-range wakefields (simplified equation of motion 8) in order to validate the analytical development previously exposed, or in the "real case" (see Eq. 7), i.e taking into account the finite bunch length as well as the single-bunch beam-breakup effects.

4.1 Experiment I

For $Q_b = 1.6$ nC, Experiment I has been simulated in the case where the first two or the first four cavities of module ACC1 are tuned to the resonant condition (Eq. 1) of the TM_{110} mode at 1875 MHz (see Fig. 5(a) and Fig. 5(b) without or with single–bunch effect respectively). Note that Fig. 5(b) can be approximatively deduced from Fig. 5(a) by a translation of 0.8 mm which corresponds to the contribution of the short-range wakefield for $Q_b = 1.6$ nC.
With a bunch charge of 8 nC, the tuning of the first only or the first two cavities of module ACC1 appears sufficient for this experiment (see Fig. 6(a) and Fig. 6(b) without or with single–bunch effect respectively). As expected, the effects of short-range wakefields are in this case multiply by a factor 8/1.6=5 (see the 4 mm displacement of the first bunch in Fig. 6(b)), giving a contribution of 4–5.5 mm to the final displacement of the bunch train (more precisely, these contributions are 4, 4.6 or 5.3 mm respectively when zero, one or two cavities are tuned to the resonant condition, the effects of long-range and short-range wakefields being not linearly additive when the multi-bunch instability becomes large, compare Fig. 6(a) and Fig. 6(b)). Finally, as announced in Subsection 3.3, note that the contribution of the long-range dipole wake is about **6 mm**, i.e. approximatively $\delta x_0/2$, for $Q_b = 8$ nC and when only the first cavity is tuned to the TM_{110} mode (see Fig. 6(a)).
To summarize, due to the rapid build up of the steady-state, a beam of about 150-200 bunches per pulse with a bunch charge of 1 to 2 nC is sufficient for this experiment.

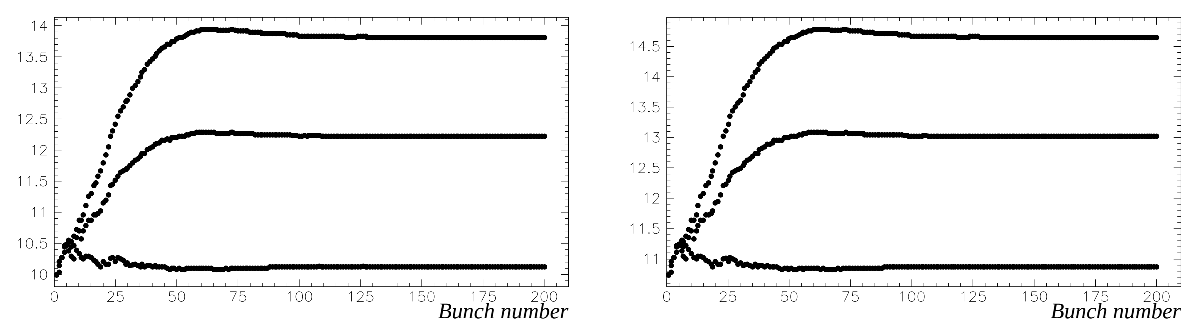

(a) (b)

Figure 5: Bunch position [mm] at the exit of module ACC1 without (a) or with (b) single-bunch beam breakup; 0, 2 or 4 cavities tuned (1.6 nC bunch charge, cavities un-powered)

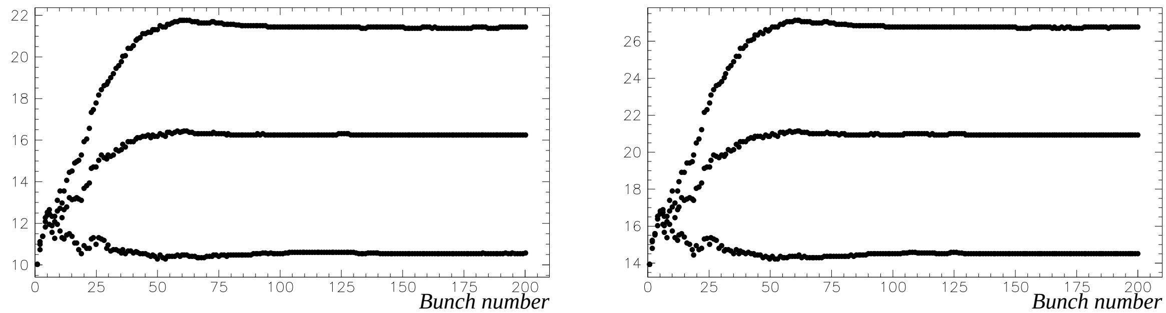

(a) (b)

Figure 6: Bunch position [mm] at the exit of module ACC1 without (a) or with (b) single-bunch beam breakup. 0, 1 or 2 cavities tuned (8 nC bunch charge, cavities un-powered)

4.2 Experiment II

We assume here the TM_{110} mode previously studied to be resonant at $\omega = 1873.84$ MHz in the first cavity of module ACC1. Therefore, by choosing the modulation frequency Ω equal to 0.16 MHz (implying $\mathcal{A}_+ = 0$ and $\mathcal{A}_- = \mathcal{A}_-^{peak}$, see Subsection 3.2), we expect that the output signal possesses a component in phase quadrature with respect to the input one, the amplitude of which is 6 and 6/5 mm for $Q_b = 8$ nC and 1.6 nC respectively, and when the short-range wakefield is artificially switched-off. As shown in Fig. 7(a) and Fig. 8(a), this is precisely what we obtain by simulation.
On the contrary, the short-range wake-fields give always an in-phase contribution to the output signal:

$$\delta x_{k,\mathrm{BPM}}^{short-range} \;\propto\; \delta x_{k,0}\,\frac{Q_b}{E_0}\left\langle W_T^\delta \right\rangle \;\propto\; \sin(k\Omega T + \phi)$$

where $\left\langle W_T^\delta \right\rangle$ represents the short-range transverse delta-function wake potential averaged over one bunch. As said in the previous subsection, the amplitude of this supplementary contribution is 0.8 mm and 4.6 mm for $Q_b = 1.6$ nC and 8 nC respectively. Therefore, the absolute amplification of the output signal (i.e $|\delta x_{k,\mathrm{BPM}} - \delta x_{k,0}|$) is expected to be equal to $\sqrt{(6^2 + 4.6^2)} \approx 7.6$ mm for a bunch charge of 8 nC (for $Q_b = 1.6$ nC, the corresponding amplification is $7.6/5 \approx 1.5$ mm) when both effects of single-bunch and multi-bunch instabilities are taken into account. These predictions are effectively reproduced by simulation as shown in Fig. 7(b) and 8(b).
In conclusion, this experiment guarantees the same measurement sensitivity as the one obtained with experiment I provided that the modulation amplitude given by the rf deflectors can be pushed to 10 mm (which corresponds to the nominal field value in the magnetic chicane constructed for Experiment I); nevertheless, since only one cavity can be tested at the same time, the bunch charge has to be taken as high as possible. Then, two different operating modes can be chosen:

- either measure the difference between the output and the input signal and subtract from it the contribution induced by the short-range wakefield which can be directly estimated from the displacement of the first bunch,

- or extract from the output signal the cosine component (i.e. the one in phase quadrature with respect to the input signal) which is practically not affected by the single-bunch wakefield and exhibits a very narrow peak at the resonance.

These two measurement methods are obviously complementary and might be successively adopted, on the one hand in order to validate the physical model used and, on the other hand, to cross-check the results obtained.

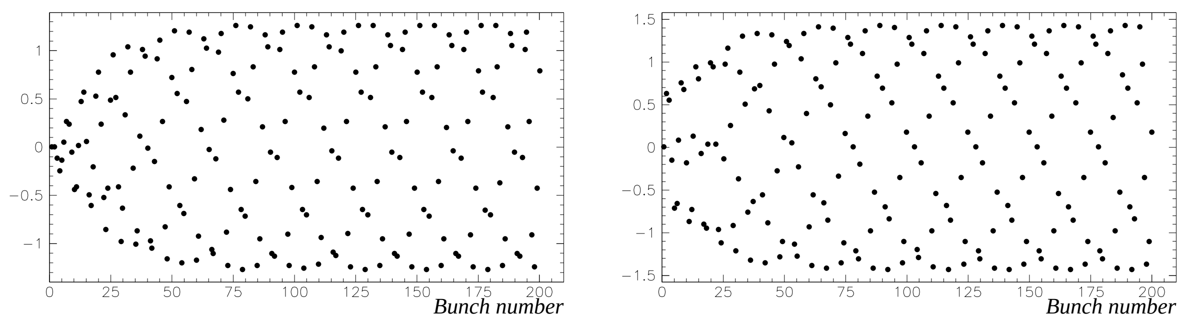

(a) (b)

Figure 7: Relative bunch displacement [mm] (i.e. difference between the output signal and the input one) at the exit of module ACC1 without (a) or with (b) single-bunch beam breakup effect. The modulation frequency Ω is tuned to the resonance condition of the TM_{110} mode at 1875 MHz of the first cavity (1.6 nC bunch charge, cavities un-powered)

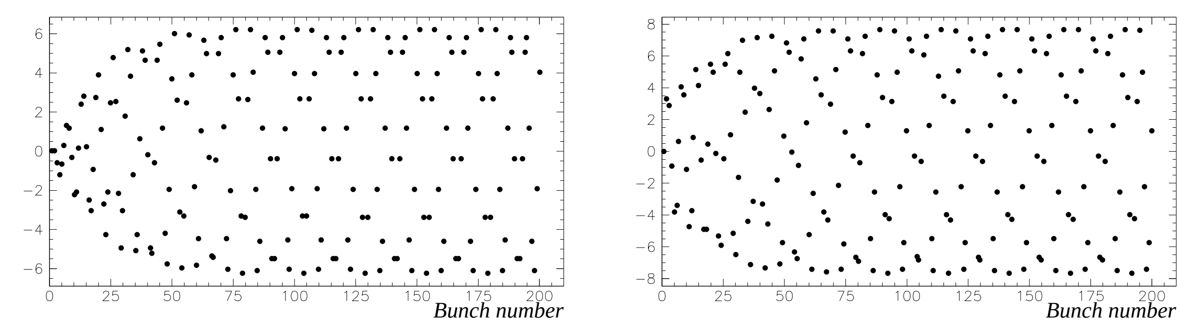

(a) (b)

Figure 8: Relative bunch displacement [mm] (i.e. difference between the output signal and the input one) at the exit of module ACC1 without (a) or with (b) single-bunch beam breakup effect. The modulation frequency Ω is tuned to the resonance condition of the TM_{110} mode at 1875 MHz of the first cavity (8 nC bunch charge, cavities un-powered)

5 Conclusion

Concerning the expected measurement sensitivity, these two experiment seem to be rigorously equivalent. The second one (Experiment II) possesses however the advantage that the cavity geometry does not need to be modified during operation; the resonant conditions are obtained by a judicious choice of the modulation of the initial bunch offset. Nevertheless, this last affirmation requires that the following conditions are respected; if ω_{i_0,j_0} represents the frequency of the dipole mode i_0 selected in the cavity number j_0, these conditions are:

$$(\omega_{i,j} + \omega_{i_0,j_0})/\omega_b \ \text{ and } \ (\omega_{i,j} - \omega_{i_0,j_0})/\omega_b \ \text{ not integer for } \ i \neq i_0 \ \text{ or } \ j \neq j_0$$

(only the second condition is required for Experiment I). If some cavity does not satisfy one of these conditions, the tuning system of the latter has to be actuated in order to avoid this kind of degeneracy and then optimize the measurement quality.
In other words, the dipole modes of each of the eight cavities of module ACC1 have to be listed before starting either one of the two experiments. Concerning the resonant dipole modes of highest impedances, this can be achieved by detecting with a spectrum analyzer the dipole HOM power generated by the off-axis bunch train and collected in both HOM couplers of the measured cavity. This work being done, if resonances observed with beam at the BPM location do not correspond to any of dipole modes previously listed, the operator will easily deduce the presence of a high impedance trapped mode: this is also the aim pursued by these two experiments.

References

[1] TESLA collaboration. *TESLA test facility linac - Design Report.* Version 1.0, March 1995, TESLA Report 95-01.

[2] A. Mosnier. *Instabilities in Linacs.* CERN 95-06, Rhodes, Greece, Sep. 1995, p. 459.

[3] V. Balakin. *Proposal for an Experiment at Tesla Test Facility.* Communication, March 1996, Protvino.

[4] A. Chao, B. Richter, C.-Y. Yao, *Nucl. Inst. Meth.*, **178** (1980) p. 1.

[5] K. J. Kim. Nucl. Instrum. Methods A **275**, 201 (1989).

[6] E.I. Jury. *Theory and Application of the Z-Transform Method.* NY, J. Wiley & Sons, 1964.